

State-of-Charge Estimation Using Electrochemical Battery Model for Electric Vehicles

Ahmet Akbulut*

Ankara University, Ankara, Turkey

Abstract: The Battery Management System design is one of the most up-to-date topics of electric vehicles and alternative energy systems today. Battery behavior changes over time as the number of charge/discharge cycles increases and aging effects. In order to ensure long battery life and maintain its performance, the Battery Management System must monitor the battery status correctly. To do this, there is a need for a model that accurately expresses the battery dynamics. In this study, three filters were used for estimation of State of Charge using electrochemical model. These filters have been tested using 10 different drive cycle speed profiles. The results were evaluated considering the need for filter performances to be operable on a vehicle.

Keywords: Battery management system, driving model, electrochemical model, kalman filter, state of charge

Received: 03 December 2017; **Accepted:** 05 January 2018; **Published:** 12 February 2018

I. INTRODUCTION

In automotive applications, a battery system consists of a battery and a Battery Management System (BMS). The BMS includes hardware and software units that control charging and discharging to ensure safe operation. It also performs the functions of thermal management of the battery pack and the balancing of the voltages of the cells. Lithium-Ion (Li-ion) batteries appear to be the best solution when compared to other technologies with energy-weight ratios, no memory effect, low self-discharge, and small internal resistance. The ever-decreasing costs also make them the leading solution candidates for automotive applications. One of the important parameters for the safe charging and discharging of the battery is the State of Charge (SOC). The BMS identifies the condition of the battery at the moment of operation and ensures that it can be safely charged and discharged at an appropriate level to improve its service life. However, SOC measurement cannot be done directly. Instead, it must be derived by measuring battery voltage, current, and other battery information. Accurate estimation of SOC value can prevent battery damage, rapid wear, and overcharging/over-discharging.

As the behavior of the battery can change over time,

its performance will also change over time. Accordingly, it is necessary to extend the service life. To design a BMS software algorithm, a model describing the battery dynamics is required. The main task of the BMS software is to monitor the physical parameters while observing the condition of the battery as the battery ages. In general, a BMS uses the equivalent circuit models as a model. However, these models have limited ability to predict the state of the battery when compared to electrochemical models. Voltage and current are evaluated as a function of time for the analysis of the battery condition. Processing of collected data can be done for various purposes and in various ways. The data can be compared with a characteristic pattern obtained experimentally from the battery. Or a mathematical model can be given as an input to describe the characteristic behavior of the battery. The open circuit voltage of the battery is also tried to be calculated from this data. Ideally, the parameters of these models are related to all the battery characteristics about the desired information. The open circuit voltage method and the amperage counting method can lead to incorrect evaluations due to the complex and challenging operating conditions of the cars. For example, the battery voltage may reach a stable state

*Correspondence concerning this article should be addressed to Ahmet Akbulut, Department of Electrical and Electronics Engineering, Ankara University Ankara, Turkey E-mail: aakbulut@ankara.edu.tr

© 2018 KKG Publications. All rights reserved.

at the end of a long rest period, the open circuit voltage should ideally be measured when the battery voltage is stable. It is difficult for the battery pack to reach a stable voltage condition in a short period of time, due to frequent charging and discharging, large-scale changes in current, and their effect on the battery voltage. The correct initial SOC value should be entered for the amperage counting method. Again, vehicle working conditions limit this, too. The current battery condition may not be obtained when the car is started. Electrochemical reactions in the battery set also cause noise that cannot be neglected to get over the data during measurement. Higher order or full electrochemical models can predict the solid concentration profile for electrode and electrolyte, but long calculation times and extreme model complexity are not suitable for real-time estimation/control applications. Reduced battery models are more suitable for model-based applications.

II. LITERATURE REVIEW

The studies in the literature for battery models can be grouped into four main categories. These are physical (electrochemical), statistical, analytical, and electrical equivalent circuit models. Statistical models are based on extracting meaningful structures from data sample sets rather than deriving from the basic physical data and laws, and the parameters to be used when creating the model [1, 2]. These models are compact and fast, but not as accurate as physical models. Probabilistic modeling is based on data interpretation similar to statistical modeling. In these methods, the behavior of the battery is not a specific physical process, but the parameters are defined as a probabilistic process based on statistical results [3]. Modeling the batteries as equivalent circuits does not yield results with sufficient accuracy. In these types of models, there is a possibility to perform mathematical calculations on the model. Equivalent circuits for charge-discharge or impedance curves are, therefore, modeled and analyzed. Equivalent circuit models have been used for parameter estimation in electric vehicles [4, 5, 6, 7, 8]. If it is desired to optimize the system by taking advantage of battery performance, it should be used for circuit simulations with a recursive optimization system. Such simulations take time and cannot respond instantly. Analytical equivalent battery models are used to avoid this situation. In this type of model, physical and statistical approaches can be said to be put together. The structure is based on the use of fewer parameters obtained with experimental results in a highly simplified physical battery model. In other words, the mathematical form of the system is derived from physical equa-

tions while the parameters are derived from “black box” experiments [9]. Physical models are based on internal chemical processes of batteries. In these models, the processes inside the battery are given in detail. The advantages of these models are that they are very accurate and robust. The disadvantages are that it is difficult to configure because it requires detailed information about the battery, and it takes a long time for the calculations because it requires the solution of a large number of differential equations. In order to avoid this problem, some assumptions were made and models of reduced order were derived. Two electrochemical models, full-order and reduced-order, are used in this study. The full model is known as the Doyle-Fuller-Newman model [10]. The reduced model is the model commonly used in the literature and experimentally validated [11, 12, 13].

III. METHODOLOGY

The study consists of four main steps. The first part involves obtaining the scenarios necessary to evaluate the performance of the algorithms. A total of 10 scenarios recommended by international organizations has been used. In the second step, the electrochemical battery model coding is done. In the third step, three filters have been implemented to perform SOC estimation. The final step involves evaluating the performance of these filters for all scenarios.

A. Electrochemical Model of the Li-ion Cell

The Li-ion battery model presented in this study is a One-Dimensional (1D)-spatial model of the battery dynamics that developed along only one axis (the horizontal x-axis) while neglecting the dynamics in the other dimensions [10, 11]. Governing equations of lithium ion cell model are given below:

Electrolyte phase:

$$\frac{\partial}{\partial x} \left(k^{eff} \frac{\partial}{\partial x} \phi_e \right) + \frac{\partial}{\partial x} \left(k_D^{eff} \frac{\partial}{\partial x} c_e \right) + J^{Li} = 0 \quad (1)$$

Boundary conditions:

$$\frac{\partial}{\partial x} \phi_e \Big|_{x=0} = \frac{\partial}{\partial x} \phi_e \Big|_{x=L} = 0 \quad (2)$$

Where ϕ_e is the potential of the electrode phase, and k^{eff} refers to the effective ionic conductivity. The current density is given by the Butler-Volmer electrochemical kinetic equation:

$$J^{Li} = a_s i_0 \left\{ \exp \left[\frac{a_s F}{RT} \eta \right] - \left[\frac{a_c F}{RT} \eta \right] \right\} \quad (3)$$

where i_0 is the exchange current density, s and c are the anode and cathode transfer coefficients, and η is the over potential.

$$\frac{\partial(\varepsilon_e c_e)}{\partial t} = \frac{\partial}{\partial x} \left(D_e^{eff} \frac{\partial}{\partial x} c_e \right) + \frac{1-t_+^0}{F} J^{Li} \quad (4)$$

Boundary conditions:

$$\left. \frac{\partial c_e}{\partial t} \right|_{x=0} = \left. \frac{\partial c_e}{\partial t} \right|_{x=L} = 0 \quad (5)$$

$$\left. \sigma^{eff} \frac{\partial}{\partial x} \phi_s \right|_{x=\delta-} = \left. \sigma^{eff} \frac{\partial}{\partial x} \phi_s \right|_{x=\delta+} = \frac{I}{A} \left. \frac{\partial}{\partial x} \phi_s \right|_{x=0} = \left. \frac{\partial}{\partial x} \phi_s \right|_{x=L} = 0 \quad (7)$$

Where ϕ_s is the solid-phase potential, σ^{eff} is the effective conductivity, A is the plate area, and I is the applied current.

$$\frac{\partial c_s}{\partial t} = \frac{D_s}{r^2} \left(r^2 \frac{\partial c_s}{\partial r} \right) \quad (8)$$

Boundary conditions:

$$\left. \frac{\partial c_s}{\partial r} \right|_{r=0} = 0 \quad \text{and} \quad \left. \frac{\partial c_s}{\partial r} \right|_{r=R_s} = \frac{-J^{Li}}{a_s F} \quad (9)$$

Where c_s Li-ion solid phase concentration and D_s is solid phase diffusion coefficient.

All these partial differential equations must be solved taking into account the boundary conditions for solid electrodes. For this, solutions have been obtained in MATLAB environment using the finite difference method and simulations have been used as real battery state values in simulations as it is the model that gives the battery dynamics in the most accurate form.

It is impossible to use this full, i.e., non-reduced, model to solve partial differential equations involving many parameters, because this process is complex and

Where L is the thickness of the microcell, c_e is the Li-ion concentration in the solution phase, ε_e is porosity, t_+^0 is the number of transfer, and D_e^{eff} is the effective diffusion coefficient.

Solid phase:

$$\frac{\partial}{\partial x} \left(\sigma^{eff} \frac{\partial}{\partial x} \phi_s \right) - J^{Li} = 0 \quad (6)$$

Boundary conditions:

computationally expensive, it cannot be used in real-time on the vehicle. It is compulsory to reduce the model in real-time applications. To reduce this complexity, it is necessary to obtain a new model by model reduction using some approximations and simplifications. In fact, the partial differential equations in the full model are a function of the particle's position along the thickness of an electrode, the radial coordinate of a particle and time, that is, x , r , and t . These equations can be solved numerically by discretization. In the reduced model, the solid particle distribution along the electrode is neglected and it is assumed that there is a single spherical solid particle and the surface is scaled to the surface area of the porous electrode. The particle represents the entirety of the selected electrode, and its radius is R_s . In this model, a single particle representing each of the anode and cathode is used. This spherical particle is divided into layers of equal thickness. A particle is divided into $M-1$ layers in the range of Δr . The net molar flow (c_{si}) is calculated by dividing the molar difference between the previous and the next layer by the sphere volume (V_i).

$$c_{si} = \frac{4D_s \delta t}{\delta r^2 (r_{i+1} + r_i)^2} \left\{ r_i^2 [c_{s_{i+1}} - c_{s_i}] - r_{i-1}^2 [c_{s_i} - c_{s_{i-1}}] \right\} \quad (10)$$

Solid concentration is then calculated to produce the terminal voltage at the solid electrolyte interface. The SOC of the battery is calculated by the spherical average concentration ($c_{s,pavg}$) in the positive electrode (for the positive electrode):

$$SOC = 100 \times \left(\frac{\theta_{pavg} - \theta_{p0\%}}{\theta_{p100\%} - \theta_{p0\%}} \right) \quad (11)$$

Discrete time state equations must be provided to implement the estimation filters. State equations are as fol-

lows:

$$c_s = A c_s + B J^{Li} \quad (12)$$

$$c_{se} = C c_s + D J^{Li} \quad (13)$$

B. Voltage and SOC Estimation

To find the current drawn from the battery and supplied to the battery, the current profile must be obtained

using the scenarios. In order to obtain the current profile, the vehicle dynamics and the mechanical and electrical (electric motor, inverter) parameters of the vehicle must be determined. By using the vehicle speed, the forces acting on the vehicle are calculated by means of the specified parameters. From here, the acceleration, torque, and current are calculated. The forces acting on the car are calculated as follows [14, 15, 16, 17]. The total force acting on the vehicle can be expressed in terms of the forward-moving force, that is, the sum of the push-

ing force and the forces that counteract the advance.

$$f_k Ma = F_{itki} - \sum F_r \quad (14)$$

Where, f_k is a value called the mass factor, which converts the rotational inertia of the rotating components to an equivalent mass. M represents the mass of the vehicle, and a represents the acceleration. The total counter forces are calculated as given below. The parameters used in the equations are given in Table 1. The parameter values used in the simulations are given in Table 2.

$$\sum F_r = MgC_y \cos(\theta) + \frac{1}{2} \rho AC_s (V - V_r)^2 + Mg \sin(\theta) \quad (15)$$

TABLE 1
THE PARAMETERS USED IN THE CALCULATION OF THE FORCES ACTING ON THE VEHICLE

f_k	Inertial mass factor	Unitless
M	Vehicle mass	kg
a	Vehicle acceleration	m/s ²
g	Gravitational acceleration	m/s ²
c_y	Rolling resistance of wheels	Unitless
θ	The slope	Degree (°)
ρ	Air density	kg/m ³
A	Vehicle front area	m ²
C_s	Drag coefficient	Unitless

TABLE 2
VEHICLE AND ELECTRICAL SYSTEM PARAMETERS USED IN SIMULATIONS

Vehicle mass (kg)	1200
Inertial mass factor	1.05
Drag coefficient	0.35
Vehicle front area	2.1
Wheel radius	0.315
Rolling resistance	0.015
Transmission gear ratio	7.4
Transmission efficiency (%)	95
Electric motor efficiency (%)	80
Inverter output (%)	80
Regenerative brake efficiency (%)	70

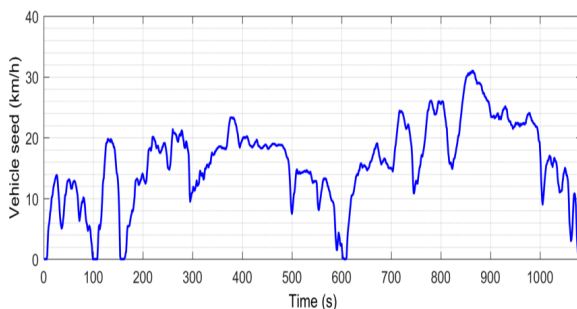


Fig. 1. ARTEMISROAD drive cycle speed profile

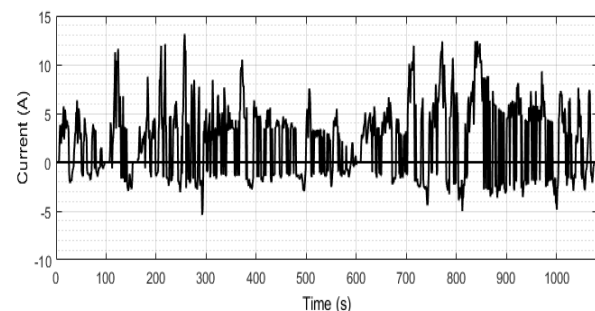


Fig. 2. ARTEMISROAD drive cycle current profile

Figures 1, 2, 3, and 4 Show the Speed and Current Profile for the ARTEMISROAD and FTPCOL Drive Cycles, Respectively.

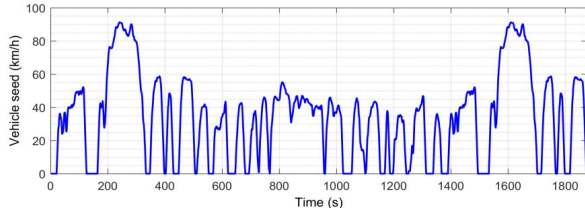


Fig. 3. FTPCOL drive cycle speed profile

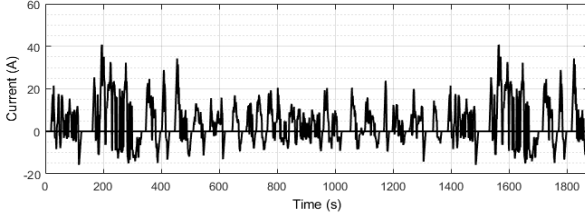


Fig. 4. FTPCOL drive cycle current profile

Since the voltage measurement model is not linear, the Extended Kalman Filter (EKF), Unscented Kalman Filter (UKF), and Smooth Variable Structure Filter (SVSF) are used as the filters.

IV. RESULTS

In this study, for the total of 10 scenarios, the current profile was obtained and full electrochemical model battery status values were calculated. Measurements were then generated by adding noise to the instantaneous battery cell voltage values obtained by using the full model for each scenario. Voltage and SOC estimation values were obtained by running the noise measurements with three different filters (EKF, UKF, and SVSF). In all simulations, the scenarios were run with the battery at a charge of 67.31%. The upper voltage limit is 4.31 V and the lower voltage limit is 3.105 V for the overcharge and discharge protection of the battery. When the upper limit is reached, the current input to the battery will be interrupted. However, applying the lower limit may mean cutting off the current for a vehicle in traffic. This can lead to undesirable situations in terms of traffic safety. On the other hand, if driving continues, the battery may be damaged. So, the decision here is to stay the driver. The BMS will alert the driver before reaching critical SOC.

TABLE 3
FILTER PERFORMANCE RESULTS FOR $M = 11$ (EKF)

Scenario	SOC Error	Calculation Time (s)
ARTEMISROAD	2.01	0.0286
ARTEMISURBAN	0.66	0.0273
EUDC	2.15	0.0112
FTPCOL	2.12	0.0513
HWFET	1.97	0.0206
IM240	0.94	0.0071
NEDC	1.48	0.0311
NYCCOL	0.56	0.0155
SC03COL	0.96	0.0161
UDDS	0.85	0.0349

TABLE 4
FILTER PERFORMANCE RESULTS FOR $M = 11$ (UKF)

Scenario	SOC Error	Calculation Time (s)
ARTEMISROAD	1.37	0.0811
ARTEMISURBAN	0.55	0.0815
EUDC	1.41	0.0306
FTPCOL	1.20	0.1357
HWFET	1.55	0.0571
IM240	0.31	0.0188
NEDC	1.09	0.0861
NYCCOL	0.33	0.0462
SC03COL	0.74	0.0434
UDDS	0.76	0.0979

As shown in Tables 3, 4, 5, the best estimation performance for all scenarios was done with UKF filter. For SOC estimation, Filters generally give relatively poor results in high-acceleration scenarios. It is observed that the calculation time of UKF is 2 to 4 times higher than the other two filters. All simulations were conducted us-

ing a computer with a 2.7 GHz processor and 16 GB of memory. As can be seen in Tables 6, 7, 8, more precise estimates are obtained when the number of discretization steps increases. However, calculation times increase by about 50%. In the SOC estimation, it is observed that the SVSF and UKF filters performed better this time.

TABLE 5
FILTER PERFORMANCE RESULTS FOR $M = 11$ (SVSF)

Scenario	SOC Error	Calculation Time (s)
ARTEMISROAD	1.59	0.0280
ARTEMISURBAN	0.61	0.0248
EUDC	1.85	0.0107
FTPCOL	1.37	0.0493
HWFET	1.77	0.0186
IM240	0.55	0.0059
NEDC	1.29	0.0315
NYCCOL	0.53	0.0142
SC03COL	0.80	0.0143
UDDS	0.77	0.0324

TABLE 6
FILTER PERFORMANCE RESULTS FOR $M = 21$ (EKF)

Scenario	SOC Error	Calculation Time (s)
ARTEMISROAD	1.49	0.0328
ARTEMISURBAN	0.57	0.0304
EUDC	1.49	0.0121
FTPCOL	1.30	0.0559
HWFET	1.72	0.0246
IM240	0.36	0.0074
NEDC	1.09	0.0362
NYCCOL	0.41	0.0192
SC03COL	0.74	0.0188
UDDS	0.76	0.0411

TABLE 7
FILTER PERFORMANCE RESULTS FOR $M = 21$ (UKF)

Scenario	SOC Error	Calculation Time (s)
ARTEMISROAD	0.29	0.1413
ARTEMISURBAN	0.16	0.1319
EUDC	0.93	0.0523
FTPCOL	0.35	0.2427
HWFET	0.48	0.0909
IM240	0.57	0.0319
NEDC	0.32	0.1532
NYCCOL	0.13	0.0739
SC03COL	0.34	0.0791
UDDS	0.32	0.1802

TABLE 8
 FILTER PERFORMANCE RESULTS FOR $M = 21$ (SVSF)

Scenario	SOC Error	Calculation Time (s)
ARTEMISROAD	1.19	0.0303
ARTEMISURBAN	0.46	0.0274
EUDC	0.90	0.0126
FTPCOL	1.14	0.0571
HWFET	1.31	0.0251
IM240	0.34	0.0069
NEDC	0.80	0.0363
NYCCOL	0.25	0.0166
SC03COL	0.56	0.0174
UDDS	0.70	0.0379

V. DISCUSSION & CONCLUSION

In this study, SOC and voltage estimates were obtained with three different filters for various speed profiles. It is seen that EKF and SVSF filters can be preferred when considering the necessity of working in real time. However, with the UKF, more accurate estimates have been obtained. Estimation accuracy increases when the number of discretization steps used in the battery model is increased. Design should be made by making a trade-off between calculation time and accuracy. From the results obtained, it is also evaluated that it would be beneficial to provide driving advice for the driver according to the condition of the battery.

ACKNOWLEDGMENT

This study was supported by TUBITAK with Grant Nr. 115E080. The author would like to express their gratitude to this institution for their support.

REFERENCES

- [1] C. Krintz, Y. Wen, and R. Wolski, "Application-level prediction of battery dissipation," in *Proceedings of the 2004 International Symposium on Low Power Electronics and Design*, Newport Beach, CA, 2004.
- [2] N. A. Mahardiono and I. Djunaedi, "Piecewise affine modelling of hybrid control systems in solar cell-battery-supercapacitor," *Journal of Advances in Technology and Engineering Research*, vol. 1, no. 1, pp. 35–39, 2015. doi: <https://doi.org/10.20474/-jater1.1.5>
- [3] V. Rao, G. Singhal, A. Kumar, and N. Navet, "Battery model for embedded systems," in *18th International Conference on VLSI Design*, Kolkata, India, 2005.
- [4] C. Mi, B. Li, D. Buck, and N. Ota, "Advanced electro-thermal modeling of lithium-ion battery system for hybrid electric vehicle applications," in *Conference of Vehicle Power and Propulsion*, Arlington, TX, 2007.
- [5] C. Sen and N. C. Kar, "Battery pack modeling for the analysis of battery management system of a hybrid electric vehicle," in *Conference Vehicle Power and Propulsion*, Dearborn, MI, 2009.
- [6] M. W. Verbrugge and R. S. Conell, "Electrochemical and thermal characterization of battery modules commensurate with electric vehicle integration," *Journal of the Electrochemical Society*, vol. 149, no. 1, pp. A45–A53, 2002. doi: <https://doi.org/10.1149/1.1426395>
- [7] M. W. Verbrugge and P. Liu, "Electrochemical characterization of high-power lithium ion batteries using triangular voltage and current excitation sources," *Journal of Power Sources*, vol. 174, no. 1, pp. 2–8, 2007. doi: <https://doi.org/10.1016/j.jpowsour.2007.03.019>
- [8] F. Umer and N. Cetinkaya, "Transient analysis due to short circuit faults in wind hybrid systems," *Journal of Advances in Technology and Engineering Research*, vol. 3, no. 3, pp. 89–100, 2017. doi: <https://doi.org/10.20474/jater-3.3.4>
- [9] P. Rong and M. Pedram, "An analytical model for predicting the remaining battery capacity of lithium-ion batteries," *IEEE Transactions on Very Large Scale Integration (VLSI) Systems*, vol. 14, no. 5, pp. 441–451, 2006. doi: <https://doi.org/10.1109/date.2003.1253775>
- [10] M. Doyle, T. F. Fuller, and J. Newman, "Modeling of galvanostatic charge and discharge of the lithium/polymer/insertion cell," *Journal of the Electrochemical Society*, vol. 140, no. 6, pp. 1526–1533, 1993. doi: <https://doi.org/10.1149/1.2221597>
- [11] K. Smith and C.-Y. Wang, "Solid-state diffusion

- limitations on pulse operation of a lithium ion cell for hybrid electric vehicles,” *Journal of Power Sources*, vol. 161, no. 1, pp. 628–639, 2006. doi: <https://doi.org/10.1016/j.jpowsour.2006.03.050>
- [12] D. Di Domenico, G. Fiengo, and A. Stefanopoulou, “Lithium-ion battery state of charge estimation with a kalman filter based on a electrochemical model,” in *IEEE International Conference on Control Applications*, San Antonio, TX, 2008.
- [13] R. Ahmed, M. El Sayed, I. Arasaratnam, J. Tjong, and S. Habibi, “Reduced-order electrochemical model parameters identification and soc estimation for healthy and aged li-ion batteries part 1: Parameterization model development for healthy batteries,” *IEEE Journal of Emerging and Selected Topics in Power Electronics*, vol. 2, no. 3, pp. 659–677, 2014. doi: <https://doi.org/10.1109/jestpe.2014.2331059>
- [14] L. R. Gantt, “Energy losses for propelling and braking conditions of an electric vehicle,” Ph.D. dissertation, Virginia Tech, Blacksburg, VA, 2011.
- [15] R. Garcia-Valle and J. A. P. Lopes, *Electric vehicle integration into modern power networks*. New York, NY: Springer Science & Business Media, 2012.
- [16] R. Abousleiman and O. Rawashdeh, “Energy consumption model of an electric vehicle,” in *Conference on Transportation Electrification and Expo (ITEC)*, Metro Detroit, MI, 2015.
- [17] A. Damiano, C. Musio, and I. Marongiu, “Experimental validation of a dynamic energy model of a battery electric vehicle,” in *International Conference on Renewable Energy Research and Applications (ICRERA)*, Paris, France, 2015.